

# Group-Control Motion Planning Framework for Microrobot Swarms in a Global Field

Siyu Li<sup>1</sup>, Afagh Mehri Shervedani<sup>1</sup>, Miloš Žefran<sup>1</sup>, and Igor Paprotny<sup>1</sup>

University of Illinois Chicago, Chicago IL 60607, USA  
{sli230, amehri2, mzefran, paprotny}@uic.edu

**Abstract.** This paper investigates how group-control can be effectively used for motion planning for microrobot swarms in a global field. We prove that Small-Time Local Controllability (STLC) in robot positions is achievable through group-control, with the minimum number of groups required for STLC being  $\log_2(n + 2) + 1$  for  $n$  robots. We then discuss the complexity trade-offs between control and motion planning. We show how motion planning can be simplified if appropriate primitives can be achieved through more complex control actions. We identify motion planning problems that balance the number of robot groups and motion primitives with planning complexity. Various instantiations of these motion planning problems are explored, with simulations to demonstrate the effectiveness of group-control.

**Keywords:** Micro Robots · Global Field · Control and Motion Planning.

## 1 Introduction

Microrobots have gained significant attention for their potential in medical, environmental, and industrial applications. Effective control mechanisms are crucial for enabling diverse functionalities. Various control methods have been developed to address the unique challenges faced by microrobots, including magnetic control [16, 22, 23], optical control [2, 9, 15, 19], and acoustic control [1, 10]. These systems are controlled by global fields, and as a result they are massively under-actuated.

Currently, parallel control of multiple microrobots in a global field is based on the design of robots with distinct physical characteristics, which results in different responses of each robot to the same control signal. The Global Control Selective Response (GCSR) paradigm introduced in [7, 8] relies on fabrication to make each robot respond appropriately to the control signal. Turning-rate Selective Control (TSC), introduced in [20], is a variation of GCSR and differentiates robots by explicitly designing them with different turning rates. These methods face challenges in scaling to larger swarms due to manufacturing complexities. Ensemble Control (EC), proposed by [3], leverages differences in linear velocity and turning rate parameters among robots stemming from randomness in fabrication to control the position of individual robots. Unfortunately, the ability

to control individual robots is inherently limited by noise so this approach also scales poorly.

This paper focuses on stress-engineered MEMS microrobots (MicroStressBot), originally developed in [6]. The swarm is powered by a uniform electrostatic field generated by a substrate, which means that all robots are controlled by a single global signal. Their size limits onboard control logic and power storage, making it essential to simultaneously coordinate large groups of microrobots for applications like micro-assembly or drug delivery. Our work explores the concept of on-board multi-stage Physical Finite-State Machines (PFSMs) introduced in [21]. PFSMs allow robots to be individually addressed and activated one by one. Our previous work [17] takes the idea of PFSMs further by introducing *group-based control*. In this paper, we investigate the trade-off between the complexity of motion planning and control within the *group-control* framework. In particular, we introduce several instances of control and motion planning problems and discuss their scalability.

Motion planning for microrobots involves determining a sequence of movements to achieve specific goals while avoiding obstacles and collisions. Various methods exist, including graph-based methods like Dijkstra’s and  $A^*$  search [13], sampling-based algorithms like Rapidly-exploring Random Trees (RRTs) [14] and optimization-based methods [11, 29]. Recent advances in machine learning, such as [24, 26, 27], leverage neural networks to speed up RRTs and control techniques for mobile robot navigation. Despite a wealth of solutions for motion planning problems, motion planning for microrobot swarms in a global field remains a challenging problem because the system is highly dimensional yet massively underactuated, having a single control signal.

Fundamentally, when a microrobot swarm is controlled by a global control signal, the robots can be controlled individually only when each robot responds to the control signal differently. In this paper, we introduce the *group-control* framework to differentiate the motion of each microrobot in the swarm. We prove that Small Time Local Controllability (STLC) is achievable in robot positions given an appropriate group allocation, with the minimum number of groups required for STLC being  $\log_2(n+2) + 1$  for  $n$  robots. Additionally, we discuss the complexity trade-offs between control and motion planning. We identify motion planning problems that balance the number of robot groups and motion primitives with planning complexity. Various instantiations of these motion planning problems are explored, with simulations to demonstrate the scalability and effectiveness of the proposed algorithms.

## 2 Background

### 2.1 MicroStressBot

Electrostatic stress-engineered MEMS microrobot (MicroStressBot) is a  $120 \mu\text{m} \times 60 \mu\text{m} \times 10 \mu\text{m}$  mobile microrobot platform introduced in [6]. A MicroStressBot has two actuated internal degrees of freedom (DOF): an untethered scratch-

drive actuator (USDA) that provides forward motion, and a steering-arm actuator that determines whether the robot moves in a straight line or rotates. A single MicroStressBot can have its arm either raised or lowered, depending on the voltage applied across a substrate formed by an electrode array. When high enough voltage is applied to the substrate, the arm is pulled into contact with the substrate and the robot rotates around the contact point. In contrast, when the voltage is reduced below a threshold, the arm is raised, and the robot moves forward.

MicroStressBot control has been successfully implemented in [8]. It has been shown that if the pull-down and release voltages of robots are different, they can be independently controlled. However, it is difficult to consistently manufacture the robots so that they respond in the desired way. As a result, the approach scales poorly.

## 2.2 Physical FSM Robots

One solution to dramatically improve the scalability of the microrobot swarm control is to make the robots respond to a temporal sequence of (a small number of) voltage levels rather than to the voltage directly. Finite State Machines (FSMs) can accept a set of input sequences [25] (sequences of control signal levels). Previously, in [21], we proposed the on-board MEMS Physical FSM (PFSM) that, upon the acceptance of a unique control signal sequence, causes the arm of the MicroStressBot to be pulled up or down. PFSMs can be constructed from several basic modules that are combined together and thus fabricated efficiently. In this work, we build on this idea to propose *group-control*. In particular, we use the fact that several PFSM modules, each corresponding to one group, can be combined together so each robot can belong to several groups.

## 2.3 Group-Control

The core idea of group-control is that by equipping the robots with PFSMs, they can be assigned to (several) different groups. When the activation sequence corresponding to a group is sent to the swarm, all the robots that belong to the group are activated. In this paper, a MicroStressBot being activated corresponds to its arm being pulled up so it can move forward (translate). By assigning each robot to a unique subset of groups, we can differentiate between the robots and make them respond differently to a sequence of inputs that activate all the groups one after the other, each time moving the robots belonging to the group for some distance.

Table 1 shows how six robots can be assigned to different groups. In order to make the selection of groups unique to each robot, if we have  $n$  robots, we need  $m = \log_2(n + 2) + 1$  groups ( $n + 2$  rather than  $n$  because each robot needs to belong to at least one group so it can move forward, and no robot can belong to all groups so it can rotate). We add one more group where none of the robots translate, they all rotate in place. If we have  $m$  groups, this special group will be the group  $G_m$ .

As can be easily seen from Table 1, group assignment corresponds to assigning a unique bit pattern (subset of the groups) to each robot, where each bit corresponds to a group (labeled as  $G_i$ ,  $i = 1, 2, 3$  in Table 1). Each robot then belongs to the groups where the corresponding bit equals 1. For example, robot  $R_1$  belongs to group  $G_3$ . Instead, robot  $R_3$  belongs to the groups  $G_2$  and  $G_3$ , etc. The group  $G_4$  is the group with all 0's, representing the additional group where all the robots are rotating. It is clear that this method guarantees that each robot has a distinct group allocation. Also, note that each group (apart from the added group like  $G_4$ , which contains no robots and corresponds to the case where all the robots rotate) can contain at most  $\frac{2^{m-1}-2}{2} = 2^{m-2} - 1$  robots.

Group	Robot					
	$R_1$	$R_2$	$R_3$	$R_4$	$R_5$	$R_6$
$G_1$	0	0	0	1	1	1
$G_2$	0	1	1	0	0	1
$G_3$	1	0	1	0	1	0
$G_4$	0	0	0	0	0	0

Table 1: Allocating 6 robots to 3 groups.

The group allocation can be realized by the on-board PFSM. At each time step  $k$ , only one group of robots is activated, and the robots belonging to that group translate (move forward) while the remaining robots rotate. We call a sequence of group selections an *activation sequence*.

If  $m$  is the number of groups and  $n$  is the number of robots, we would need  $k = O(\log_2 m) = O(\log_2(\log_2(n+2) + 1))$  bits to select a group through a PFSM [21]. Thus, PFSMs for group-based control can be significantly simpler than in the case when each robot needs to be selected individually.

### 3 Modeling

#### 3.1 Dynamics

To describe *group-control* mathematically, we start with a dynamic model of a MicroStressBot. The robot can move freely on a horizontal plane, so its configuration space is Euclidean group  $SE(2)$ . We will describe the state of the robot  $i$  with a vector  $[x_i, y_i, \theta_i]^T$ , where  $x_i$  and  $y_i$  are the Cartesian coordinates of the pivot point of the robot and  $\theta_i$  is the robot orientation. The equations of motion are given by:

$$\frac{d}{dt} \begin{bmatrix} x_i \\ y_i \\ \theta_i \end{bmatrix} = a_i \cdot \begin{bmatrix} \cos \theta_i \\ \sin \theta_i \\ 0 \end{bmatrix} \cdot u + (1 - a_i) \cdot \begin{bmatrix} 0 \\ 0 \\ 1 \end{bmatrix} \cdot \omega_i, \quad (1)$$

where  $a_i \in \{0, 1\}$  is the switching input that determines whether the robot is moving forward or turning in place, while  $u \in \mathbb{R}^+$  and  $\omega \in \mathbb{R}^+$  are the rates of

forward motion and rotation, respectively, where  $\omega_i = u/r_i$  with  $r_i$  being the turning radius of each robot. If the control inputs are piecewise constant over each epoch  $\Delta T$ , we obtain the following discrete-time model:

$$\begin{bmatrix} x_i(k+1) \\ y_i(k+1) \\ \theta_i(k+1) \end{bmatrix} = \begin{bmatrix} x_i(k) \\ y_i(k) \\ \theta_i(k) \end{bmatrix} + \begin{bmatrix} a_i(k) \cos \theta_i(k) \\ a_i(k) \sin \theta_i(k) \\ (1 - a_i(k))1/r_i \end{bmatrix} u(k) \cdot \Delta T. \quad (2)$$

Note that  $u$  is a unilateral control input. In other words, MicroStressBot can not go backward or turn counterclockwise.

### 3.2 Switched and Embedded Systems

Group-control corresponds to setting the switching input  $a_i$  of the robot  $i$  to 1 if it belongs to the activated group or to 0 otherwise. Group-control with  $m$  groups thus turns the swarm into a switched system with  $m$  discrete states. Such *m-switched system* has a system state  $q(t) \in \mathbb{R}^N$  that evolves according to the following dynamics:

$$\dot{q}(t) = f_{v(t)}(t, q(t), u(t)), \quad q(t_0) = q_0, \quad (3)$$

where at each  $t > t_0$ , the switching control  $v(t) \in \{1, 2, \dots, m\}$ , and the control input  $u(t) \in \mathbb{R}^M$  for some  $M$  (in our case  $M = 1$ ). In the case of  $n$  robots that move in  $SE(2)$ , we have  $N = 3n$ . The vector fields  $f_i : \mathbb{R} \times \mathbb{R}^N \times \mathbb{R}^M \rightarrow \mathbb{R}^N$ ,  $i \in \{1, 2, \dots, m\}$  are  $C^1$  and we assume that  $u(t)$  is measurable. Note that the evolution of the state  $q(t)$  governed by Eq. (3) does not experience any discontinuous jumps.

By introducing new variables  $v_i(t) \in [0, 1]$  that satisfy the constraint  $\sum_{i=1}^m v_i(t) = 1$ , the switched system (3) can be converted to the embedded form [4, 28]:

$$\dot{q}(t) = \sum_{i=1}^m v_i(t) f_i(t, q(t), u_i(t)), \quad q(t_0) = q_0, \quad (4)$$

where  $u_i$  is the control input for each vector field  $f_i$ . It can be shown [4] that the set of trajectories of the switched system (3) is a dense subset of the set of trajectories of the embedded system (4). Consequently, any trajectory in the embedded system can be approximated by the switched system to any desired accuracy, which means that the controllability of the embedded system is equivalent to the controllability of the switched system.

## 4 Controllability Analysis

In order for the robots to navigate among obstacles, the system, in general, needs to be Small-Time Locally Controllable (STLC). There are otherwise configurations in the obstacle-free configuration space  $C_{free}$  that will always lead to a collision. First, we formally define the notion of STLC that will be of interest to

this paper. Let  $q(t)$  be the combined state of the robot swarm, where all robot positions are first stacked together in a  $2n$  vector, followed by a  $n$  vector of robot orientations. Let  $p(t) = q(t)[1 : 2n]$  be the position states of the robots.

**Definition 1.** *The system is small-time locally controllable (STLC) in position states about  $p(0) = p_0, \forall p_0 \in C_{free}$ , if  $p(0) = p_0$  is contained in the interior of the reachable sets  $\mathcal{R}_{p_0}$  for all  $t > 0$ . [12]*

In Eq. (1), we assumed that the MicroStressBot  $i$  has the turning radius  $r_i$ . If each robot has a different turning radius, only two groups are needed to achieve STLC through group-based control: group  $G_1$  that translates all the robots and group  $G_2$  that rotates all the robots. Now consider the three-step primitive  $P_1 = (G_1(d), G_2(\pi r_1), G_1(d))$  where  $G_1(d)$  moves all the robots forward for  $d$ ,  $G_2(\pi r_1)$  rotates all the robots so that robot 1 rotates exactly for  $\pi$  radians, and then  $G_1(d)$  again moves all the robots forward for  $d$ , making robot 1 return to its starting position. Then the sequence  $P_2 = (P_1, G_2((\pi - \Delta\theta_2)r_2), P_1)$  moves robots 1 and 2 back to their initial position, where  $\Delta\theta_2$  is the angular displacement of robot 2 due to  $P_1$ . Iteratively,  $P_{n-1}$  moves only one robot while all the others return to the starting position. By first rotating the robot so that the resulting movement due to  $P_{n-1}$  is in the desired direction, we can clearly individually move any robot in any direction, showing that the system is STLC. Note that a similar argument has been used in [20] to introduce TSC.

Assuming that all the robots have different turning rates again shifts the burden of control to fabrication and in general scales poorly. In the rest of the paper, we thus **assume that all the robots have the same turning rate  $r$** . We will show that group-control still guarantees STLC.

*Remark 1.* Given a collection of sets of robots  $\{S_0, S_1, \dots\}$  with each  $S_i$  containing robots with the same turning rate, and  $S_i$  and  $S_j$  having different rates if  $i \neq j$ , STLC can be achieved by combining the approach above with group-control that will be described below within each set.

#### 4.1 Unilateral Control to Bilateral Control

As stated above, in the rest of the paper, we only consider the case when all the robots have the same turning radius  $r$ . In [17], we showed that a swarm of MicroStressBots under group-control is (globally) controllable (even without using the group where all the robots rotate). However, we were not able to demonstrate that the system is STLC. In this paper we show that by adding the group where all the robots rotate, STLC can be achieved.

One of the challenges to show that our system is STLC is that the robots are controlled unilaterally. In other words, they can only move forward but not backward. Similarly, they can rotate clockwise but not counter-clockwise. This is the result of the fact that the control input  $u$  in Eq. (4) is positive. We show that this restriction can be relaxed.

We return to the switched system in Eq. (1). Let

$$q(t) = [x_1, y_1, x_2, y_2, \dots, x_n, y_n, \theta_1, \theta_2, \dots, \theta_n]$$

be the state of the swarm, where  $q(t) \in \mathbb{R}^{3n}$ . We can see that  $q(t)[1 : 2n]$  are the *position states*, with  $q(t)[2j - 1 : 2j]$  representing the position of robot  $j$ . Also,  $q(t)[2n + 1 : 3n]$  are the *orientation states*, where  $x(t)[2n + j]$  is the orientation of the robot  $j$ . Next, let  $\alpha_i = [\alpha_{i,1}, \dots, \alpha_{i,n}]^T, i = 1, \dots, m$  be the activation vector corresponding to group  $i$  being activated. In other words,  $\alpha_{i,j} = 1$  if robot  $j$  belongs to group  $i$ , and 0 otherwise. The overall swarm dynamics can then be written as:

$$\dot{q}(t) = f_{\nu(t)}(q(t)) \cdot u(t) \quad u(t) \in \mathbb{R}^+ \quad (5)$$

where  $\nu(t) \in \{1, \dots, m\}$ , and for each  $i$ ,  $f_i$  is obtained by choosing  $a_j = \alpha_{i,j}$  in Eq. (1). This equation describes a switched driftless control-affine system [5, 18].

We introduce the notion of induced vector fields  $g_i$  and  $h_i$  so that  $f_i = g_i + h_i$ . Here,  $g_i$  contains only the position states information and  $h_i$  contains only the orientation states information. Given that  $G_m$  is the group where all the robots rotate, and the rotation radius of all of them is equal, let  $f_m(\pi)$  represent the rotation of all robots by  $\pi$  radians using the rotation-only vector field.

**Proposition 1.** *The control sequence  $(f_i(d), f_m(\pi), f_i(d), f_m(\pi))$ , where  $f_i(d)$  corresponds to the activation of group  $G_i$  so the robots in the group translate for  $d$ , corresponds to a vector field  $h_i(\frac{2d}{r})$  that rotates the robots that do not belong to the group  $i$  by  $\frac{2d}{r}$  and keeps the rest of the robots where they were.*

*Proof.* Observe that  $f_i(d)$  translates the robots that belong to  $G_i$  for  $d$  without changing their orientation, and rotates the robots that do not belong to  $G_i$  for  $\frac{d}{r}$ . The application of  $f_m(\pi)$  rotates all the robots for  $\pi$ , which means that the robots that belong to the group  $G_i$  now point in the opposite direction. The second application of  $f_i(d)$  then brings the robots that belong to  $G_i$  back to their initial position, while adding another  $\frac{d}{r}$  to the orientation of the robots that do not belong to  $G_i$ . Finally,  $f_m(\pi)$  rotate the robots in  $G_i$  to their original orientation. The robots not in  $G_i$  have instead rotated in total for  $\frac{2d}{r} + 2\pi = \frac{2d}{r}$ .  $\square$

*Remark 2.* Observe that for any angle  $\theta \in [0, 2\pi]$ ,  $h_i(-\theta) = h_i(2\pi - \theta)$ . The orientation vector field  $h_i$  is thus bilateral.

Once we have the orientation vector field  $h_i$ , we can easily obtain the translation vector field  $g_i$ :

**Proposition 2.** *The control sequence  $(f_i(d), h_i(-\frac{d}{r}))$  corresponds to a vector field  $g_i(d)$  that translates the robots in  $G_i$  for  $d$  and leaves all the other robots where they were.*

*Remark 3.* We can also easily see that  $(f_m(\pi), g_i(d), h_i(\pi)) = g_i(-d)$ . Thus, the translation vector field  $g_i$  is bilateral.

Note that while  $h_i$  rotates the robots that are not in  $G_i$  in place, the other robots travel back and forth and could potentially collide with an obstacle. However, we can restrict the motion of the robots in  $G_i$  to a small ball of the radius

$\epsilon$  and apply  $h_i(\frac{\epsilon}{r})$  multiple times to obtain the desired rotation of the robots not in  $G_i$  without the robots in  $G_i$  leaving a small neighborhood of their initial location.

Technically, the rotations we used in the constructions above can not be performed in zero time. However, for the purpose of position control, they can be assumed to take place instantaneously. Therefore, in the rest of the paper, we can safely assume that the control input can be bilateral.

With the construction above, the original embedded system in Eq. (4) with unilateral vector fields  $\{f_i, \dots, f_m\}$  becomes an embedded system with **bilateral** vector fields

$$\mathcal{F} = \{g_1, \dots, g_{m-1}, h_1, \dots, h_{m-1}\}. \quad (6)$$

## 4.2 Control of Robot Orientation

We have showed that each group  $G_i$  induces a vector field  $g_i$  that just translates the robots in the group, and a vector field  $h_i$  that just rotates the robots that are not in  $G_i$ . What we show next is that we can independently control the orientation of  $m$  robots:

**Proposition 3.** *The orientation of any  $m$  robots can be controlled to any desired orientation  $(\theta_1, \dots, \theta_m)$ .*

Note that the rest of the swarm will rotate in place to some orientation that can not be directly controlled.

To illustrate this proposition, consider the rotation vector fields  $g_1, \dots, g_{m-1}$  in (6) and the additional original rotation-only vector field  $f_m$ . All of these vector fields can rotate the robots without translating them. The proposition can then be proved by observing that using these vector fields, the orientations of the robots linearly depend on the arguments (rotation angles) of these vector fields. For example, for the 4-group case in Table 1, we get the equation:

$$\begin{bmatrix} 1 & 1 & 1 & 0 & 0 & 0 \\ 1 & 0 & 0 & 1 & 1 & 0 \\ 0 & 1 & 0 & 1 & 0 & 1 \\ 1 & 1 & 1 & 1 & 1 & 1 \end{bmatrix}^T * [u_1 \ u_2 \ u_3 \ u_4]^T = q[2n+1 : 3n] - q[2n+1 : 3n](0) \quad (7)$$

where  $q[2n+1 : 3n]$  are the orientations of the robot after the application of the vector fields, and  $q[2n+1 : 3n](0)$  are their initial orientations.

It is easy to see that for  $m$  groups, the rank of the matrix that appears in the equation above is  $m$ . This means that  $m$  of the  $n$  equations can be solved exactly for the desired inputs  $u_i$ .

## 4.3 Small-Time Local Controllability (STLC)

After we have identified the control vector fields in Eq. (6), we can proceed to show that the swarm is STLC in positions. Traditionally, we can do this by analyzing the closure of  $\mathcal{F}$  under the Lie bracket operation. However, we will show



that we can independently translate any robot in arbitrary direction without moving any other robot. This shows that the system is STLC in positions.

Suppose that we want to independently translate some robot  $k \in \{1, \dots, n\}$ . Let  $G_{\hat{k}}$  be any group that contains the robot  $k$ . Let  $\text{Rot}_{i_1, \dots, i_m}(\theta_1, \dots, \theta_m)$  correspond to setting the orientation of robots  $i_1, \dots, i_m$  to  $\theta_1, \dots, \theta_m$  as described above. Also, assume that the members of the group  $G_{\hat{k}}$  are robots  $l_1, \dots, l_j, k$ .

We can then state the following:

**Proposition 4.** *The control sequence  $P_1(d) = (h_{\hat{k}}(d), \text{Rot}_{l_1, \dots, l_m}(\pi, \dots, \pi), h_{\hat{k}}(d))$  only translates robots  $l_{m+1}, \dots, l_j, k$ .*

*Proof.* Observe that under the control sequence above, the first  $m$  robots in  $G_{\hat{k}}$  will travel back and forth while the rest of the robots in the group will undergo some translation.  $\square$

Once we have the control sequence  $P_1$ , it is easy to see that a control sequence  $(P_1(d), \text{Rot}_{l_{m+1}, \dots, l_{2m}}(\pi, \dots, \pi), P_1(d))$  will only translate robots  $l_{2m+1}, \dots, l_j, k$ . By repeating this process we can therefore eliminate translation of all the robots  $l_1, \dots, l_j$  except for the robot  $k$ . Of course, we can always rotate the robot  $k$  appropriately so that the final translation is in the desired direction, showing that each robot can be translated independently, and that the system is STLC in positions.

## 5 Motion Planning

After we have shown that the swarm of MicroStressBots under group-control is STLC, we consider the motion planning problem for the swarm. Given our proof of STLC the problem is not how to move the swarm to a particular configuration, but how to move it **efficiently**. In other words, ideally we would like the robots to move to their desired configuration in parallel and not one by one. But planning such parallel motion directly is fraught with significant complexity due to the high dimension of the configuration space and the fact that we have a single control input. We have determined that effective motion planning for the global group control in high-dimensional state spaces should involve the design of motion primitives with **subgroups**.

The objective of designing motion primitives is to divide a robot group into smaller subgroups, each containing fewer robots. These primitives simplify the motion planning task by reducing the coupled motions in the group. We present primitives described by Lie bracket motions, as the higher the order of the Lie brackets, the fewer robots belong to it. It is important to note that, in this paper, these subgroups are logical constructs apart from  $\log(n+2)+1$  number of physical groups. However, these logical groups can be physically manufactured to increase the number of physical groups, thereby enhancing control capabilities. Fig.1 shows the trade-offs between the complexity of control and planning. The order of Lie bracket  $r_k$  is used to quantify the complexity. As we construct motion planning based on a higher order  $r_k$ , the control realizing  $r_k$  order Lie

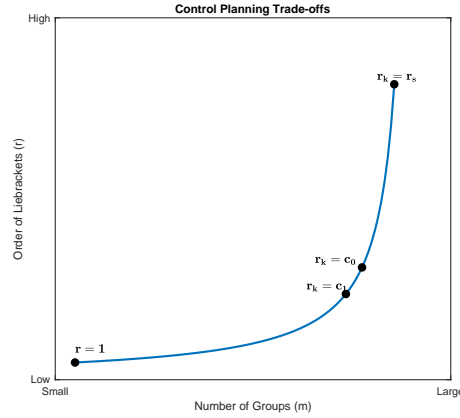


Fig. 1: An illustration of control and motion planning complexity trade-offs.  $r_k = 1, r_s, c_1, c_0$  represent four cases: pure planning, pure control, controlling rotations, and decoupled subgroup, respectively.

brackets become more complex, while increasing the number of decoupled subgroups simplifies the planning (curve from left to right).

In the following section, we discuss the complexity of motion planning through a formal abstraction of various levels of motion planning problems. Subsequently, we simulate the motion planning instantiations to demonstrate that the constructed subgroups can effectively reduce planning time.

### 5.1 Motion Planning Approximation Scheme

We start by giving some assumptions and definitions that are fundamental to the group-robot motion planning problem. Several **assumptions** are provided below.

- Robots are controlled by a global signal that operates them in groups, with one group activated at a time.
- A predefined map of the area is available and known.
- Each robot is assigned a starting point and a destination. The starting point includes the robot’s position and orientation, whereas the destination does not consider orientation.

**Definition 2. Motion Primitive:** *Unlike the groups encoded in the robot’s physical finite state machine (FSM) structure, a subgroup is a logical construct. A subgroup contains fewer robots that all move forward when the subgroup is involved. This abstraction will allow us to formulate the motion planning problem in layers of increasing difficulty. Physically, the motion induced by the subgroup corresponds to a particular Lie bracket and can thus be physically realized. When using a motion primitive associated with a subgroup  $p$  we will use the notation  $\langle p, l \rangle$  to indicate that the robots in the subgroup  $p$  moved forward for the distance  $l$ .*

**Definition 3. Primitive Order** The order of a primitive corresponding to the subgroup  $p$  is the order of the Lie bracket used to realize it. The order of the Lie bracket is the number of generators from the set of vector fields  $\mathcal{F}$  in Eq. (6) in it. In general, the higher the order of a Lie bracket, the fewer the number of robots move under that bracket. However, there is no one-to-one correspondence between the Lie bracket order and the number of robots it affects, as this also depends on the variety of rotation vector fields used to compute the Lie bracket. Fundamentally, the order of the Lie bracket indicates the difficulty of its implementation, while the number of robots affected by it reflects the complexity of the motion planning.

**Definition 4. Motion Planning Problem Abstraction** The motion planning problem for  $n$  robots of level  $r$ , denoted as  $\mathcal{M}_s^g(n, r)$ , corresponds to the problem of finding a collision-free trajectory (sequence of motion primitives) for  $n$  robots controlled by a global field from some initial state  $s$  to a goal state  $g$ , where the motion primitives that are used have the primitive order at most  $r$ .

**Proposition 5.** Consider the motion planning problem  $\mathcal{M}_s^g(n, r_k)$  for  $n$  robots, and  $r_k \leq r_s$ , where  $r_s$  is the primitive order required for moving each individual robot (the highest order of the Lie bracket needed to prove STLTC). If  $r_1 < r_2 \leq r_s$ , the complexity of the motion planning problem  $\mathcal{M}_s^g(n, r_2)$  is less than  $\mathcal{M}_s^g(n, r_1)$ . Initially, when  $r_k = r_s$ , the complexity of the motion planning problem  $\mathcal{M}_s^g(n, r_s)$  is linear in robot number. Moreover, for any other  $r_k$ , the complexity of motion planning problem  $\mathcal{M}_s^g(n, r_k)$  has a loose upper bound  $o(nL^{r_s-r_k})$ , assuming moving along the first order Lie bracket has a constant complexity  $L$ .

*Proof.* We calculate the complexity by abstracting the planning problem for multiple robots by moving each of them sequentially using the  $r_s$  order of the Lie bracket. Initially,  $r_k = r_s$ , there is only one robot contained in each Lie bracket. The complexity in this case is linear in the number of robots since moving one robot to the goal takes constant time. Secondly, when  $r_k = r_s - c$ , each Lie bracket contains multiple robots. Moving only one robot is equivalent to moving in the  $c$ -th order Lie bracket given  $r_k$  order Lie brackets as controls. Thus, the complexity is calculated as  $o(\mathcal{M}) = o(nL^c) = o(nL^{r_s-r_k})$ . In the real world, planning for multiple robots occurs simultaneously, so we consider this complexity as a loose upper bound.  $\square$

*Example 1.* Continuing with the example of 6 robots with 4 groups, consider the motion planning problem  $\mathcal{M}(n = 4, r_k = 3)$  where the minimum order to move each robot is  $r_s = r_k = 3$ . Further, we select six primitives at the highest order Lie brackets that move each robot individually, as shown in Table.2. The problem  $\mathcal{M}(4, 3)$  reduces to rotating each robot to the goal and then moving it using its corresponding primitive. Since this plan for each robot takes constant time, the complexity of the motion planning problem  $\mathcal{M}(4, 3)$  is linear in the number of robots.

For the motion planning problem  $\mathcal{M}(n = 4, r_k = 2)$ , choosing the primitive at the first order Lie brackets. Each primitive moves two robots simultaneously;

for example  $[h_2, g_1]$  moves robot 4 and 5 sideways and  $[h_2, g_3]$  moves robot 1 and 5 sideways. To move each robot individually, the sequence of primitives must mimic the higher-order Lie brackets. For instance, robot 1 is moved in the direction of Lie bracket  $[h_1, [h_2, g_3]]$  using a sequence of primitive chosen from  $[h_2, g_3]$  and  $h_1$ . Thus, moving one robot requires a complexity of  $o(L^{3-2}) = o(L)$  and the overall complexity for  $\mathcal{M}(4, 2)$  is  $o(nL)$ .

Lie brackets	Robot
$[h_1, [h_2, g_3]]$	$-c_1, -s_1$
$[h_1, [h_3, g_2]]$	$-c_2, -s_2$
$[h_1, [h_3, g_2]] - [h_2, [h_2, g_1]]$	$-c_3, -s_3$
$[h_3, [h_2, g_1]]$	$-c_4, -s_4$
$[h_1, [h_2, g_3]] - [h_1, [h_1, g_3]]$	$-c_5, -s_5$
$[h_3, [h_2, g_1]] - [h_2, [h_2, g_1]]$	$-c_6, -s_6$

Table 2: The min order Lie brackets move along each individual robot. In the right column, only then nonzero elements of each Lie bracket the vector field are shown;  $c_i$  and  $s_i$  correspond to  $\cos \theta_i$  and  $\sin \theta_i$  respectively, where  $\theta_i$  is the orientation of robot  $i$ .

In short, motion planning is simplified if each robot moves sequentially; however, this approach sacrifices path optimality. The complexity of motion planning increases exponentially as robots get coupled in groups, but this trade-off for parallelism results in more optimal paths.

## 5.2 Instantiations of motion planning problem

The motion planning problem  $\mathcal{M}(n, r_k)$  addresses a class of problems involving  $n$  robots with primitives at most  $r_k$  order. Problems within this class are not unique but share the same complexity. In this section, we will discuss the instantiation of  $\mathcal{M}(n, r_k)$ .

For a given set of  $n$  robots, we use  $m$  group to control it. Depending on the chosen group allocation, the set of all primitives up to order  $r_k$  is defined as  $\mathcal{P}^{r_k} = \{f_j, S^{r_i}(\mathcal{F})\}$ , where  $j = 1, \dots, m$  and  $i \leq r_k$ . This set includes the original  $m$  groups and any additional subgroups up to  $r_k$ -th order Lie brackets. One instantiation of the motion planning problem can devise its own primitives set from complete set  $\mathcal{P}^{r_k}$ .

Next, several interesting motion planning instances are discussed to time complexity and optimality trade-offs.

**Extreme case 1: Pure planning problem** In this scenario, there are no devised primitives, and the control input is the switch between groups and linear input  $u$ . Fig.2(a)(d) shows a random run path for allocating 5 robots in 4 groups. The environment setup is a  $20 \times 20$  square environment with fixed start positions  $[0, 2; 0, 4; 0, 6; 0, 8; 0, 9]^T$  and goal positions  $[4, 4; 7, 7; 10, 10; 12, 12; 14, 14]^T$ . Circular obstacles are designed in two scenarios with radii 2 and 1, respectively.

The path is solved by MATLAB optimization (Fmincon) for a given path length  $k = 60$ , with the cost function of minimizing total control effort  $\sum_{i=1}^k u$ . The random walk collision avoidance algorithm is based on our previous work [17]. This simulation effectively demonstrates that the rotation-only group guides all robots to turn away from obstacles. The simulation is within a minute, but as the number of robots increases, the optimization, as well as random walk obstacle avoidance is no longer time-efficient.

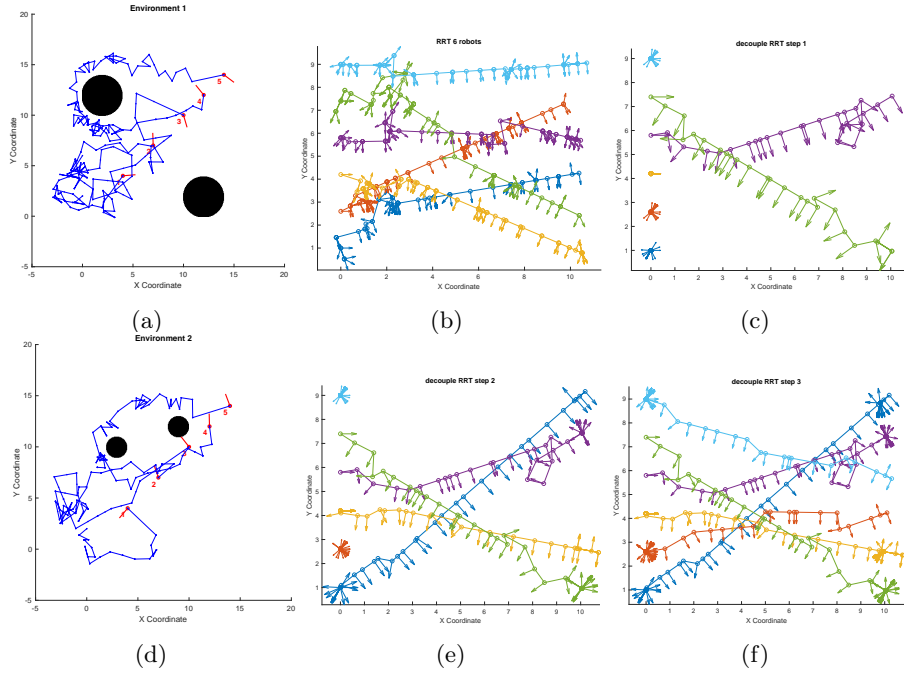


Fig. 2: (a)(d)Pure control using Fmincon and random walk obstacle avoidance. (b) Intermediate case 3: RRT using primitives at most order 3 (c), (e) and (f) Intermediate case 4: RRT 3-steps decouple subgroups

**Extreme case 2: Pure control problem** The planning problem involves guiding robots one by one using Lie bracket motions. In this case, the primitives are  $r_s$  order Lie brackets that move only one robot at a time. In this case, the planning is trivial, and what is important is how primitives can be implemented. Two ways of primitives implementation:

- Repeated Fmincon.
- Hand-designed primitives.

In the top three figures in Fig.3, Fmincon approximates  $[h_3, g_1]$  for a short distance 0.2 with path length  $k = 35$ . Then, we rotate robots 4 and 5 to their

initial orientation. Next, the Fmincon path is repeated, allowing robot 4,5 to continue to move in the goal direction. The repeated path with each length  $k = 35$  is used to get a path around robots' neighborhood.

We define the hand-designed primitives as a 3-step control  $P_1 = (f_i, rot(\pi), f_i)$ , where  $f_i$  is the vector field of group  $i$  in Eq.(5) and  $rot(\pi)$  can rotate up to  $m$  robots. As the example in Fig.3,  $f_1 = [\mathbf{0}_6, \cos_4, \sin_4, \cos_5, \sin_5, \cos_6, \sin_6, \mathbf{0}_6]$  and  $rot(\pi)$  rotate the robot 6 for  $\pi$ .  $P_1$  is the primitive for moving robots 4 and 5. In general, if more than  $m$  robots need to be rotated, we can use a nested design  $P_j = (P_j - 1, rot(\pi), P_j - 1)$ .

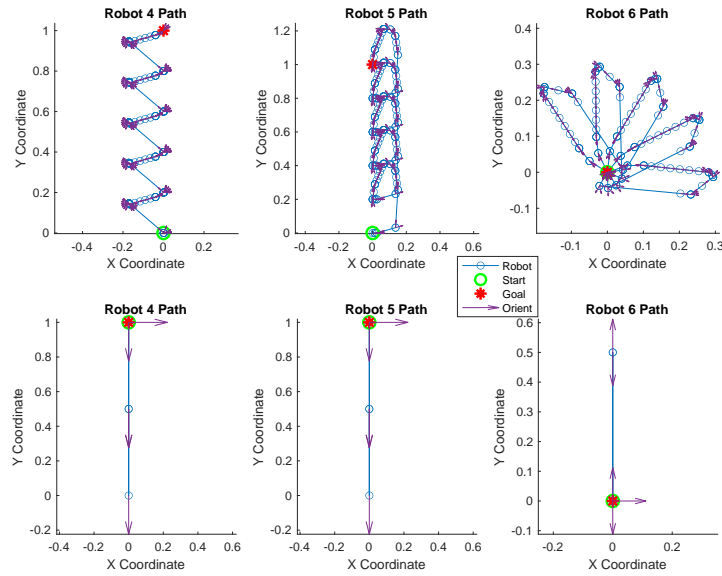


Fig. 3:  $[h_3, g_1]$ . Top: repeated Fmincon; Bottom: hand-designed primitives

All robots start at the origin and orient to the positive x-axis. Compared with the repeated Fmincon method, nested primitives provide a much simpler path. Also, solving the high dimension of Fmincon faces difficulties. Thus, we state that our designed nested primitives is a better solution.

**Intermediate case 3: Controlling rotations** When the order of primitive  $r_k \geq c_1$ , the number of robots in a subgroup is no more than  $m$ , we can control robot angles in that subgroup. Fig. 4(a) gives an example RRT planning using  $\mathcal{P}^{c_1}$  primitives for 6 robots with 4 groups. The local planner in RRT is to rotate robots in a primitive and then move forward these robots. Initially, robots are deployed in the range  $y = [0, 10]$  along the  $x = 0$ , and the final states are along  $x = 10$  with the y-axis positions randomly shuffled. The RRT stops when a goal

neighborhood of radius 0.2 is reached. The experiment was repeated 5 times with an average planning time of 72.54 seconds.

**Intermediate case 4: Decoupled subgroups** Further increasing the primitive order to  $r_k = c_0$ , several primitives can contain a distinct set of robots, and several subgroups together include all robots. Thus, we will plan each distinct subgroup sequentially. This effectively reduces the dimensionality of planning problems. Again, 6 robots with 4 groups are shown in Fig.2(c)(e)(f), where 6 robots were divided into 3 subgroups using Lie brackets  $[h2, g1]$ ,  $[h1, g3]$  and  $[h3, g2]$ . Compared with Fig.2(a), the average planning time shrinks down to 7.44 seconds under the same RRT parameters. Therefore, Decoupled subgroups should be used to deal with large size of swarms.

Next, we demonstrate three levels of motion planning for 4 robots and compare their runtime in Fig.4. Observing the path and runtime data in Tab.3, the running time decreases as we introduce more complex primitives. In particular, the pure planning RRT stops when arriving at the goal neighborhood radius of 2.5, which is far away from the goal, but still takes hundreds of times excessive time compared to the case using a primitive. It shows that RRT does not work unless we introduce subgroups. And there is a balance between robot parallelization and planning time.

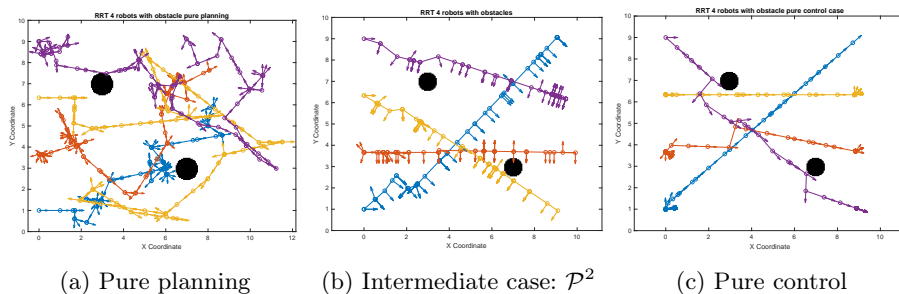


Fig. 4

Table 3: Ave Runtime and Tree Nodes for Cases

Case	Ave Runtime	Ave Tree Nodes	Neighborhood radius
Fig.4(a)	35.33 minutes	10583 nodes	2.5
Fig.4(b)	23.46 seconds	148.20 nodes	0.5
Fig.4(c)	4.10 seconds	20.75 nodes	0.5

## 6 Conclusion

In conclusion, this paper introduces a novel group-control framework for microrobot swarms in a global field, demonstrating that Small-Time Local Controllability (STLC) is achievable with the minimum number of groups being  $\log_2(n + 2) + 1$  for  $n$  robots. By balancing the complexity of the number of subgroups with motion planning, we have shown that group-control simplifies the motion planning process and scales effectively for larger swarms. Simulations confirm the framework's effectiveness, suggesting significant potential for applications in various fields requiring precise microrobot coordination. Future work will explore more complex scenarios, larger swarm sizes, and the integration of machine learning methods.



## References

1. Aghakhani, A., Pena-Francesch, A., Bozuyuk, U., Cetin, H., Wrede, P., Sitti, M.: High Shear Rate Propulsion of Acoustic Microrobots in Complex Biological Fluids. *Science Advances* **8**(10), eabm5126 (2022)
2. Banerjee, A.G., Chowdhury, S., Losert, W., Gupta, S.K.: Real-time Path Planning for Coordinated Transport of Multiple Particles using Optical Tweezers. *IEEE Transactions on Automation Science and Engineering* **9**(4), 669–678 (2012)
3. Becker, A., Onyuksel, C., Bretl, T., McLurkin, J.: Controlling Many Differential-drive Robots with Uniform Control Inputs. *The International Journal of Robotics Research* **33**(13), 1626–1644 (2014)
4. Bengea, S.C., DeCarlo, R.A.: Optimal Control of Switching Systems. *Automatica* **41**(1), 11–27 (2005)
5. Bullo, F., Lewis, A.D.: Geometric Control of Mechanical Systems, Texts in Applied Mathematics, vol. 49. Springer (2004)
6. Donald, B.R., Levey, C.G., McGray, C.D., Paprotny, I., Rus, D.: An Untethered, Electrostatic, Globally Controllable MEMS Micro-Robot. *Journal of Microelectromechanical Systems* **15**(1), 1–15 (Feb 2006)
7. Donald, B.R., Levey, C.G., Paprotny, I.: Planar Microassembly by Parallel Actuation of MEMS Microrobots. *Journal of Microelectromechanical Systems* **17**(4), 789–808 (Aug 2008)
8. Donald, B.R., Levey, C.G., Paprotny, I., Rus, D.: Planning and Control for Microassembly of Structures Composed of Stress-engineered MEMS Microrobots. *The International Journal of Robotics Research* **32**(2), 218–246 (2013)
9. Hu, W., Ishii, K.S., Ohta, A.T.: Micro-assembly Using Optically Controlled Bubble Microrobots. *Applied Physics Letters* **99**(9) (2011)
10. Jeong, J., Jang, D., Kim, D., Lee, D., Chung, S.K.: Acoustic Bubble-based Drug Manipulation: Carrying, Releasing and Penetrating for Targeted Drug Delivery Using an Electromagnetically Actuated Microrobot. *Sensors and Actuators A: Physical* **306**, 111973 (2020)
11. Karaman, S., Frazzoli, E.: Sampling-based Algorithms for Optimal Motion Planning. *The international journal of robotics research* **30**(7), 846–894 (2011)
12. Kawski, M.: The combinatorics of nonlinear controllability and noncommuting flows. In: *Mathematical Control Theory, ICTP Lecture Notes*, vol. VIII, pp. 224–311. Abdus Salam Int. Center for Theoretical Physics, Trieste (2002)
13. LaValle, S.M.: Planning algorithms. Cambridge university press (2006)
14. LaValle, S.M., Kuffner, J.J.: Randomized Kinodynamic Planning. *The International Journal of Robotics Research* **20**(5), 378–400 (May 2001)
15. Li, J., Liu, W., Li, T., Rozen, I., Zhao, J., Bahari, B., Kante, B., Wang, J.: Swimming Microrobot Optical Nanoscopy. *Nano Letters* **16**(10), 6604–6609 (2016)
16. Li, J., Li, X., Luo, T., Wang, R., Liu, C., Chen, S., Li, D., Yue, J., Cheng, S.h., Sun, D.: Development of a Magnetic Microrobot for Carrying and Delivering Targeted Cells. *Science Robotics* **3**(19) (Jun 2018)
17. Li, S., Žefran, M., Paprotny, I.: Group-based control of large-scale micro-robot swarms with on-board physical finite-state machines. In: *2022 IEEE 18th International Conference on Automation Science and Engineering (CASE)*. pp. 524–530. IEEE (2022)
18. Liberzon, D.: Switching in systems and control. Springer Science & Business Media (2003)

19. Palagi, S., Singh, D.P., Fischer, P.: Light-controlled Micromotors and Soft Micro-robots. *Advanced Optical Materials* **7**(16), 1900370 (2019)
20. Paprotny, I., Levey, C., Wright, P., Donald, B.: Turning-rate selective control : A new method for independent control of stress-engineered mems microrobots. In: *Robotics: Science and Systems*. vol. 8, pp. 321–328 (2013)
21. Paprotny, I., Zefran, M.: Finite state machine (FSM) addressable MEMS micro-robots: a new paradigm for controlling large numbers of mems microrobots. In: *2017 International Conference on Manipulation, Automation and Robotics at Small Scales (MARSS)*. pp. 1–6. IEEE (2017)
22. Pawashe, C., Floyd, S., Sitti, M.: Modeling and Experimental Characterization of an Untethered Magnetic Micro-robot. *The International Journal of Robotics Research* **28**(8), 1077–1094 (2009)
23. Qiu, F., Nelson, B.J.: Magnetic Helical Micro-and Nanorobots: Toward Their Biomedical Applications. *Engineering* **1**(1), 021–026 (2015)
24. Qureshi, A.H., Miao, Y., Simeonov, A., Yip, M.C.: Motion Planning Networks: Bridging the Gap between Learning-based and Classical Motion Planners. *IEEE Transactions on Robotics* **37**(1), 48–66 (2020)
25. Sipser, M.: Introduction to the Theory of Computation. *ACM Sigact News* **27**(1), 27–29 (1996)
26. Strudel, R., Pinel, R.G., Carpentier, J., Laumond, J.P., Laptev, I., Schmid, C.: Learning obstacle representations for neural motion planning. In: *Conference on Robot Learning*. pp. 355–364. PMLR (2021)
27. Wang, J., Chi, W., Li, C., Wang, C., Meng, M.Q.H.: Neural RRT\*: Learning-based Optimal Path Planning. *IEEE Transactions on Automation Science and Engineering* **17**(4), 1748–1758 (2020)
28. Wei, S., Uthaichana, K., Žefran, M., DeCarlo, R.A., Bengea, S.: Applications of Numerical Optimal Control to Nonlinear Hybrid Systems. *Nonlinear Analysis: Hybrid Systems* **1**(2), 264–279 (2007)
29. Zucker, M., Ratliff, N., Dragan, A.D., Pivtoraiko, M., Klingensmith, M., Dellin, C.M., Bagnell, J.A., Srinivasa, S.S.: Chomp: Covariant Hamiltonian Optimization for Motion Planning. *The International journal of robotics research* **32**(9-10), 1164–1193 (2013)